The Journal of Anatomical Sciences
Email: anatomicaljournal@gmail.com

J. Anat Sci 14(1)

Brain Morphology and Microscopic Studies on the Striato-Pallidal Nuclei of an African Rodent Species; *Thryonomys swinderianus* (African Grass Cutter)

Ivang AE[1*], Bauchi ZM[1], Agbon AN[1], Oladele SB[2].

[1]Neuroanatomy and Neuroscience Research Unit, Department of Human Anatomy, Faculty of Basic Medical Sciences, Ahmadu Bello University (ABU), Zaria-Nigeria.
[2]Department of Veterinary Pathology, Faculty of Veterinary Medicine, ABU, Zaria

Corresponding Author: Andrew I

E-email: aeivang2012@gmail.com; +2348063813875

ABSTRACTS

Thryonomys swinderianus (African grasscutter, AGC) is a breeding species widely spread across Sub-Sahara Africa and recently reported as potential model in neuroscience researches. Striato-pallidal (caudate-putamen, CPu, and globus pallidus, GP) nuclei are subcortical structures that play critical roles including planned voluntary movements in mammals. Hence, elucidating certain regions of AGC brain is critical in understanding the neurobiology of the species. This study described the brain morphologic features and characterized striato-pallidal microscopic features of AGCs. Four AGCs were obtained from a farm in Zaria. AGCs were euthanized, fixed-perfused and the brains harvested for morphologic (brain features and dimensions) and microscopic examination (histological features using H&E stains, and Nissl substances using Cresyl fast violet stain) of striato-pallidal regions. CPu was characterized into six-defined quadrants, and histometric features of the fascicules were analyzed. AGC brains were milky in color with sulcal depressions. AGC mean brain weight was greater than 11g and brain length (rostro-caudal) greater than 45mm. Microscopically, section through the cerebrum revealed a subcortical striatum with distinct CPu and GP. These nuclei revealed varying neuronal cells types and glial cells. CPu demonstrated pockets of white mater patches (fasciculi), with varying sizes and abundance across the quadrants. Histometric analysis of fasciculi within the characterized six quadrants showed difference ($p<0.05$) between quadrants, with higher values on the medial compartments when compared with lateral compartments of CPu. The brain morphologic and striato-pallidal microscopic features of the AGC is typical for a rodent species. These findings present AGC as a potential model in neuroscience related investigations.

Keywords: Brain dimension, Caudate-putamen, Globus pallidus, Histology, White-mater patches.

INTRODUCTION

The brain as the part of the central nervous system is critically involved in the integration, coordination, and regulation of major functions in a biological system. [1][2][3][4] Certain regions of the brain have been associated with distinct functions including voluntary and involuntary activities. [5][6] In the telencephalic region, cortical and subcortical structures have been associated with regulation of activities ranging from, but not limited to sensory, movement, cognition, and executive functions. [7][8][9] [10] [11] The striatum as a subcortical structure consists of majorly of two nuclei; caudate and putamen, nucleus accumbens, [12] [13] manifesting as a single complex nucleus (caudate-putamen) (CPu) in rodent species. [14] The striatum or CPu serve as a major input source for the basal ganglia of the whole brain. [15] [16] [17] The CPu together with other nuclei (globus pallidus (GP), subthalamic, and substantia nigra) largely control voluntary skeletal movements, learning and memory, reward and motivation, and emotionality. [18] [19] [20] [21] [22] Investigations using experimental animal models especially mammals including primate, non-primate, and commonly, rodents have been beneficial in biomedicine for elucidating certain pathologies related basal nuclei (striatal and pallidal) dysfunctions. [23] [24] [25] [26]

Certain under-explored African rodent species could be of benefit in neuroscience related research. [27] The African grasscutter (AGC) (*Thryonomys swinderianus*) is a breeding species widely spread across Sub-Saharan Africa. [28] [36] In West Africa, Nigeria, these species (AGCs) live in most habitats from the rain forests of the Southern regions to the semi-arid part of the extreme Northern regions of the country. [28] [29] They are herbivores, feeding on aquatic grasses in the wild [30] and in agricultural areas, feed on crops in cane plantations. [30] [31] The African grasscutter (AGC) also referred to as giant cane rat [32] has demonstrated unique behavioral patterns; being a quick runner and skilled swimmer, and using its forelimbs for eating, fighting, mating, [33] [34] and freezing on sighting its predictor. [35] This rodent can live up to seven years in captivity. [30] Description of the neurobiology of this indigenous species as potential models in research is trending amongst neuroscientists. [36] [34] Therefore, elucidating the characteristics of CPu and GP of this species is pertinent in understanding it's neurobiology, hence its significance in biomedical and clinical related investigations.

This study described the brain morphologic and striato-pallidal microscopic features of the *Thryonomys swinderianus* (African grasscutter, AGC).

MATERIALS AND METHODS

Experimental Animals: A total of four (4) adult *Thryonomys swinderianus* (African Grass-cutter, AGCs) were obtained for the study. The AGCs were procured from the Tamqua Farm in Zaria, Kaduna State, Nigeria. AGCs were transported in ventilated wooden cages to the Animal House of the Department of Human Anatomy, Faculty of Basic Medical Sciences, College of Medical Sciences, Ahmadu Bello University (ABU), Zaria and housed under standard laboratory conditions, fed with cane-sugar, water-melon, and carrots. AGCs were allowed to acclimatize for few days before

commencement of the study. AGCs were handled according to the Ethical Guidelines for the Use of Animals in Research as established by the National Committee for Research Ethics in Science and Technology (NENT).

Animal Euthanasia and Sample Collection: At the end of the acclimatization period, AGCs were weighed to determined absolute body weight using a digital weighing scale (CAMRY EK5055, Indian) before anesthesia under chloroform. The anesthetized AGC was placed on a dorsal recumbence position on a dissection board, and perfused via cardiac puncture using 10% Buffered Formol Saline fixative according to the method described by. [37]

Immediately after the perfusion fixation, the AGCs were decapitated at the atlanto-occipital joint and the head dissected by skinning and stripping off all the scalp and facial muscles followed by craniotomy to extract the whole brain. The meninges and underlying blood vessels were carefully dissected out to expose the intact brain. The harvested whole brain was observed for morphologic features and subsequently post fixed (in the same fixative for 72 hours) for microscopic assessments (Figure 1).

Morphological Studies: Morphological observations were conducted on the dorsal, lateral and ventral surfaces of the harvested whole brain. Morphometric parameters including the brain weight and dimensions were determined. Brain weight was measured using a portable digital weighing scale (Notebook Series Digital Scale, China; 0.01g). The brain dimensions were measured using a digital Vernier caliper (150 mm, China). The following dimensions were measured from the dorsal and lateral surfaces of the brain as described by [38]: (a) Brain length: an anteroposterior dimension; from the most rostral (anterior) aspect (part) of the olfactory bulb to the most caudal (posterior) part of the cerebellum; (b) Cerebral length: an anteroposterior dimension; from the most rostral aspect of the cerebrum (bulbo-cerebral junction; that is, the junction between the base of the olfactory bulb and the apex of the cerebrum) to the most caudal aspect of the cerebrum (at the cerebro-cerebellar junction); (c) Mid-antero-frontal width: (Fronto-parietal Junction; that is, the junction between the frontal and parietal lobes); (d) Cerebral width: a transverse dimension; the most prominent aspect of the cerebrum on the right and left; (e) Cerebellar length: an anteroposterior dimension; from the most rostral aspect of the cerebellum (cerebro-cerebellar junction) to the most caudal aspect of the cerebellum; (f) Cerebellar width: a transverse dimension; the most prominent aspect of the cerebellum on the right and left; (g) Cerebral dorso-ventral length: the most prominent aspect of the cerebrum from the dorsal to the ventral surface; (h) Cerebellar dorso-ventral length: the most prominent aspect of the cerebellum from the dorsal to the ventral surface. (*See* Figure **2**).

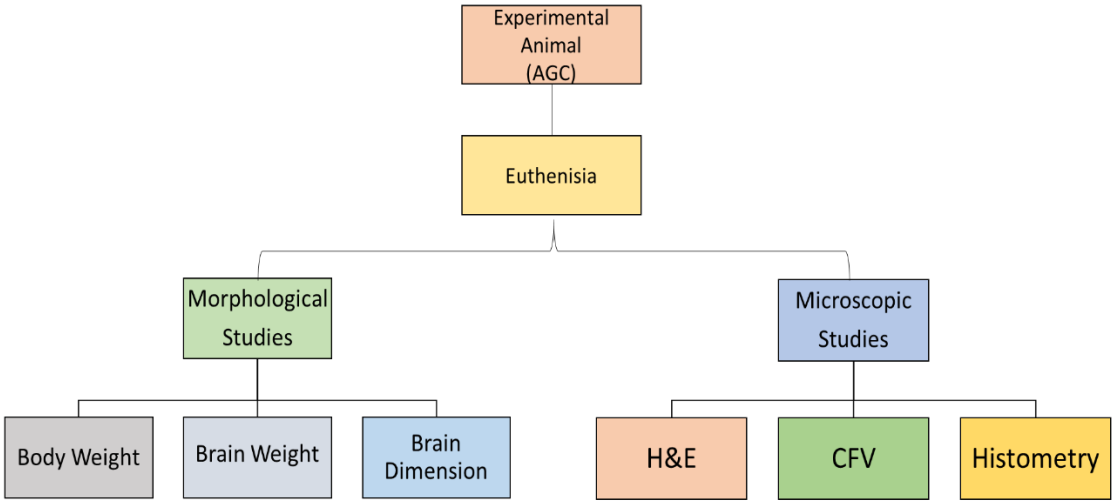

Figure 1: Experimental protocol

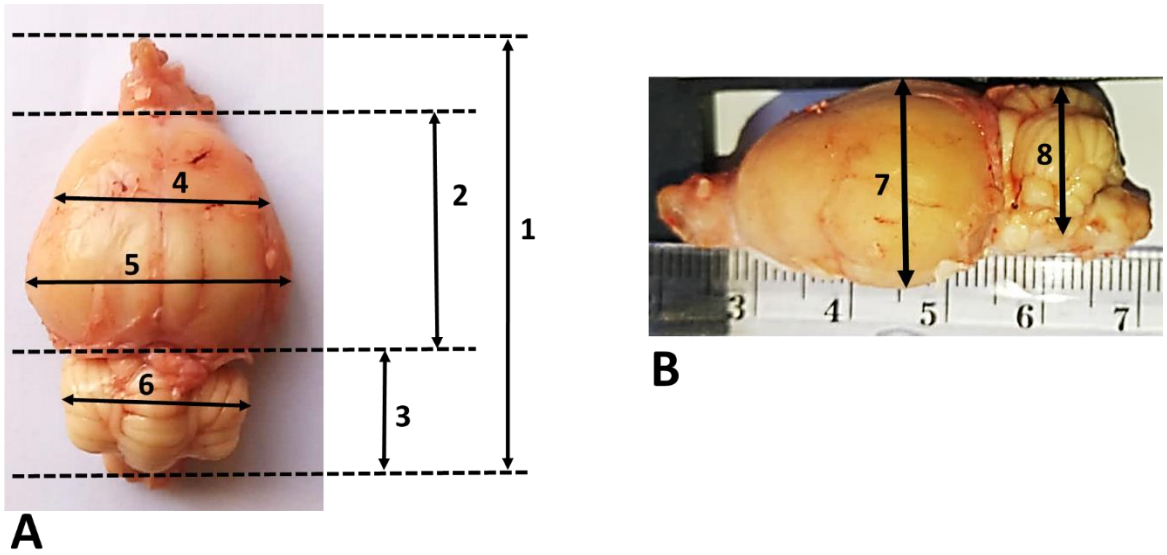

Figure 2: Morphological dimensions of the dorsal and lateral surfaces of AGC brain

A: Dorsal surface **B**: Lateral surface; **1**: Brain length (rostro-caudal); **2**: Cerebral length; **3**: Cerebellar length; **4**: Fronto-parietal transverse dimension; **5**: Cerebral width or transverse Dimension; **6**: Cerebellar width or transverse dimensions; **7:** Cerebral dorsoventral length; and **8:** Cerebellar dorsoventral length

Microscopic Studies: The post fixed brain specimens were processed using histological techniques for microscopic assessments using histological, histochemical and histometric techniques. A brief description of the protocols adopted are as follows:

Histological studies: The brain specimens were sectioned coronally to target the subcortical structures; the striatal (caudate-putamen, CPu) and pallidal (globus pallidum, GP) nuclei (*See* Figure 3). Paraffin histological sections were processed and stained with Hematoxylin and Eosin (H & E) stains to demonstrate general histoarchitectural features of CPu and GP. The histological tissue processing was carried out in the Histology Unit of the Department of Human Anatomy, ABU, Zaria. Processed tissue slides were examined using a dissecting microscope (AmScope- Stereomicroscope, China) and bright field microscope (HX-LUX Leitz Wetzlar, Germany) at different microscopic magnifications (×10, ×40, ×100, and ×250). The dissecting microscope at ×10 magnification, was used to map out or localize the entire periphery of the CPu on the coronal brain section. For the convenience of characterization of histological features, the CPu was divided into six (6) quadrants (superomedial, superolateral, mediomedial, mediolateral, inferomedial, and inferolateral) with the aid of three (3) imaginary lines (a vertical and two transversely oriented lines) (*See* Figure 3).

Each quadrant of the CPu was observed at higher magnification (×100, and ×250) for cytoarchitectural features including cell types, shapes and white mater reticulations. Similarly, the histological features of the Gp was examined at varying microscopic magnifications and cytoarchitectural features including cellular morphology were determined. Microphotograghs of the CPu and Gp were captured using a digital microscopic camera (AmScope MA-500, USA) and subsequently used for histometric assessments. Micrography were carried out in the Microscopy and Stereology Laboratory, Department of Human Anatomy, ABU, Zaria.

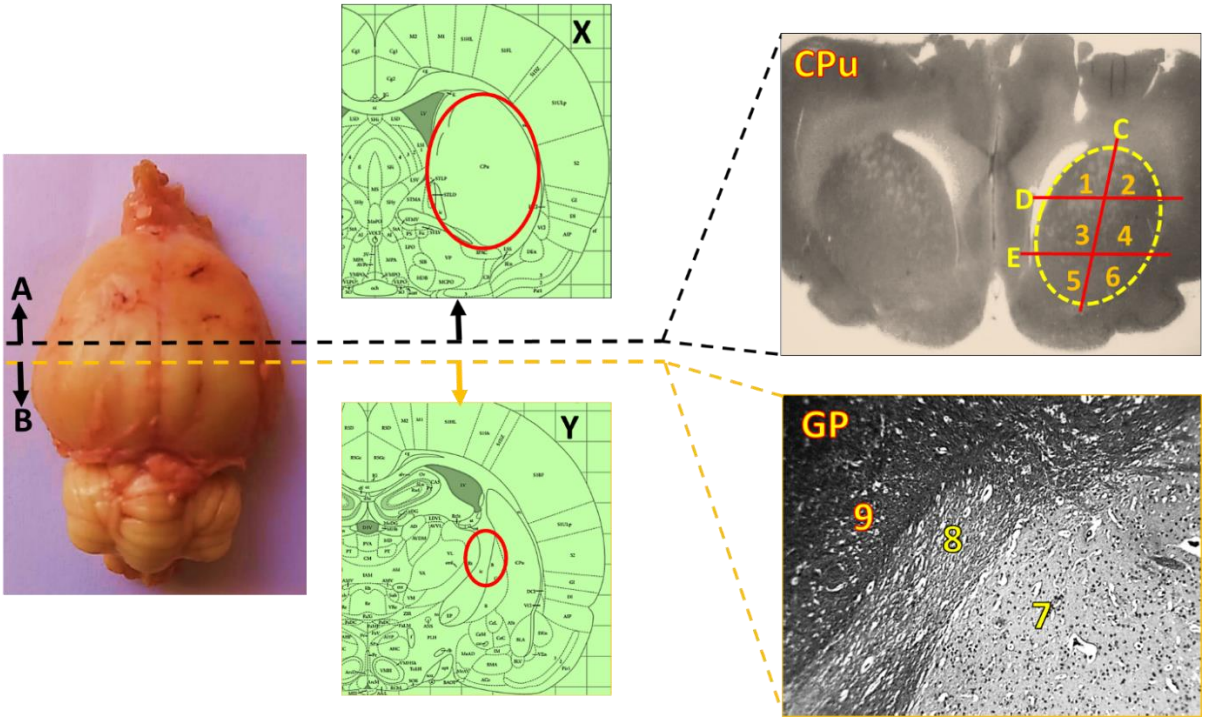

Figure 3: Coronal sections through the cerebrum of AGC to target the striatum (caudate putamen (CPu) and globus pallidus (GP)

A: Transverse or (coronal) section through CPu; B: Transverse or (coronal) section through GP; **C**: Vertical line through the midpoint of the CPu; **D**: Transverse plane through superior 1/3 of CPu; **E**: Transverse plane through inferior 1/3 of CPu; **1**: Superomedial; **2**: Superolateral; **3**: Mediomedial; **4**: Mediolateral; **5**: Inferomedial; **6**: Inferolateral; **7**: Globus pallidus; **8**: Internal capsule; **9:** Reticular thalamic nucleus; **Red oval line**: showing the CPu **(X)** and GP regions **(Y)**, *Adopted from George Paxinos and Charles Watson Rat Atlas 6th edition 2007.*

Histochemical Studies: Processed paraffin histological sections were stained with histochemical stain; Cresyl fast violet (CFV) stain to demonstrate varying neuronal cells types (and Nissl substances). Histochemical sections were examined at varying magnifications using light microscope and micrographs captured for subsequent analyses. The histochemical tissue processing was carried out in the Histology Unit, Department of Human Anatomy, ABU, Zaria.

Histometric Studies: Histometric analysis was conducted according to method described by Agbon *et al.* [81] for 2D quantification of size of structures on micrographs. Measurements were performed to estimate the sizes of fascicules/ fasciculi (white-mater reticulations) embedded within the parenchyma of CPu at the defined quadrants in AGCs.

Histometry was conducted using a light microscope with a ×10-objective lens (×100 microscopy) and a computer running image analysis software (AmScope MT version 3.0.0.5, USA) for microscopy, and digital micrographs of CPu sections stained with CFV. The AmScope imaging software polygon tool was used to measure the areas and perimeters of selected fasciculi.

Selection criterion; fasciculi within a predetermined inclusion frame/area: 136.21× 62.15µm^2 (*See* Figure 4). The mean values of measurements were computed and statistically compared between the quadrants of CPu.

Data Analysis: Data obtained were analyzed using the statistical software, GraphPad Prism (v 9.1.0, Boston, USA) and results presented in charts expressed as mean ± S.E.M. The presence of significant difference among means were determined using one-way ANOVA with Tukey *post hoc test* for significance. Confidence interval was set at $p< 0.05$.

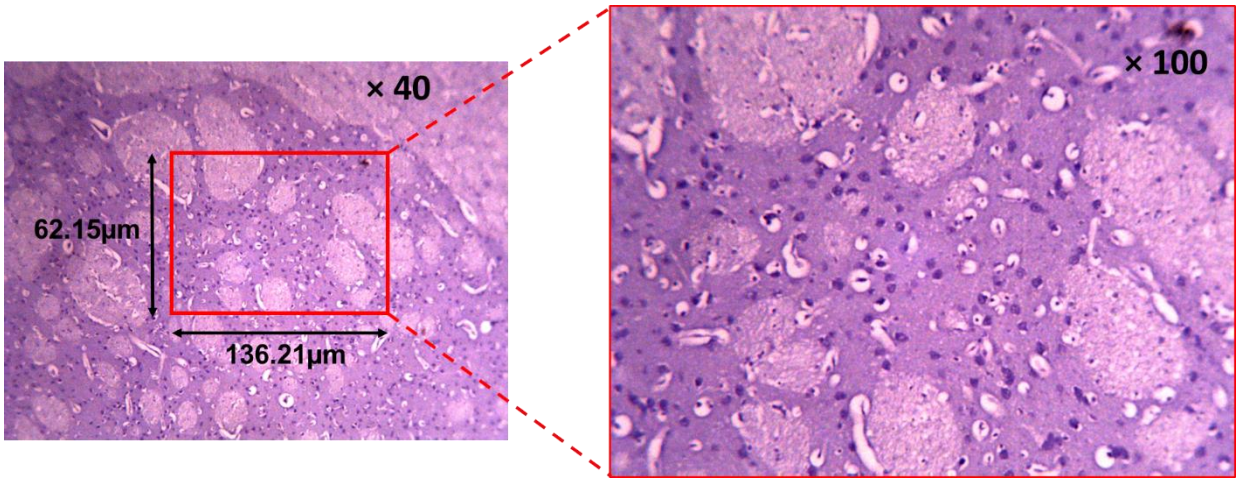

Figure 4: Sections of the Caudate putamen of AGC showing selection frame for Histometry. (H&E)

RESULTS

Morphological Assessments: The absolute body weight of AGCs revealed a mean weight of 2243.5 ±22.50 g (Table 1). Brains of the rodents were observed to be milky in color and presented with two major sulcal depressions on the dorsal surface; a coronal plane-oriented depression, separating the cerebrum (fore brain) from the cerebellum (hind brain) and the other, a sagittal plane-oriented depression, separating the cerebrum into two hemispherical halves. Minor (sulcal) depressions (grooves) were observed on the dorsal surface of each halve of the cerebral hemispheres of the AGCs. The ventral surface presented with distinct parts of the brain including the optic chiasma just rostral (anterior) to the midbrain. Other brain stem structures (pons and medulla) are delineated by depressions, the medulla continues caudally with the spinal cord. Moreover, vasculatures and other related features were observed (Figure 5).

Data on brain dimensions revealed the mean AGCs brain weight was greater than 11 g. The mean values of other AGCs brain

parameters measured are presented on Table 1.

Histological and Histochemical Assessments: Coronal section through caudate-putamen (CPu) at varying microscopic magnifications revealed distinct histoarchitectural features of the AGCs. At a lower magnifying power, a bilateral oval shaped nucleus in the subcortical regions. The CPu is related medially to the lateral walls of the lateral ventricles and corpus callosum whose fibers runs medial and superiorly to the CPu. The fibers of the corpus callosum continues supero-laterally, delineating the CPu from the cortical regions (figure 6).

At a higher microscopic power, the CPu revealed varying cell types including neuronal and glial cells, reticulations (clusters of white mater patches or fascicules) with varying shapes, sizes, and abundance. Blood vessels (capillaries) of varying sizes were observed to accompany the reticulations on the periphery. A comparison of the histoarchitectural features across the characterized quadrants of the CPu revealed no observable differences in the distribution cells (neuronal and glial). Generally, the reticulations present with a well-defined outline, relatively oval to circular shaped architecture. The sizes and abundance of these fascicules differ across the quadrants of the CPu; Fascicules appeared to be larger in the superomedial quadrant and smaller in the inferolateral when compared to that of other quadrants. Fascicles appeared to be more abundant in the lateral quadrants than in the medial quadrants generally (Figures 7).

A closer examination of the CPu cytoarchitectural features revealed distinct cell morphologies including stellate, pyramidal, horizontal, multipolar, and fusiform cell types. Glial cells were observed to be related to fascicules in a unique fashion within the parenchymal and periphery of the fascicules. Additionally, cells of CPu reacted positively with the histochemical stain, Cresyl Fast Violet (Figure 8).

Coronal sections through the globus pallidus (GP) at varying magnifying power revealed characteristic features of the subcortical nuclei, GP. At a lower magnifying power, a distinct nuclei just adjacent to the CPu; situated inferomedially lies the GP. Medially, the GP is related to the internal capsule and reticular thalamic nucleus. At a higher magnification, the GP demonstrated typical features of nervous tissues including neuronal and glial cells with related vasculatures (blood capillaries). Additionally, pockets of clustering neuronal cells were observed. Histochemical staining of GP sections with Cresyl Fast Violet revealed positive reactivity which is characteristic of neural tissue, and distinct cell morphologies including fusiform, stellate, oligodendrocyte, and pyramidal cells (Figure 9).

Histometric Analysis: Histometric characterization of the fasciculi size within the defined six quadrants of CPu revealed differences. The mean area of fasciculi in quadrant 1 was remarkably higher compared to quadrants 4, 5 and 6. The mean fasciculi perimeter within the medial quadrants presented with larger sizes ($p<0.05$) when quadrant 1 was compared to quadrants 5 and 6 (Figures 10 and 11).

Table 1: Morphological Parameters of AGCs

Parameter	Mean ± SEM
BWT (g)	2243.5 ± 22.50
BrWT (g)	12.385 ± 0.295
BL-RC (mm)	50.965 ± 0.215
CL (mm)	20.08 ± 0.530
CbL (mm)	15.985 ± 0.535
FPTD (mm)	22.74 ± 0.490
CTVD (mm)	26.055 ± 0.305
CbWTD (mm)	11.95 ± 0.50
CDVL (mm)	17.775 ± 0.925
CbDVL (mm)	11.49 ± 0.26

BWT (Body weight); **BrWT** (Brain weight); **BL-CR**: Brain length (rostro-caudal); **CL**: Cerebral length; **CbL:** (Cerebellar length); **FPTD**: (Fronto-parietal transverse dimension); **CTVD**: (Cerebral width or transverse Dimension); **CbWTD**: (Cerebellar width or transverse dimensions); **CDVL: (**Cerebral dorsoventral length); and **CbDVL: (**Cerebellar dorsoventral length).

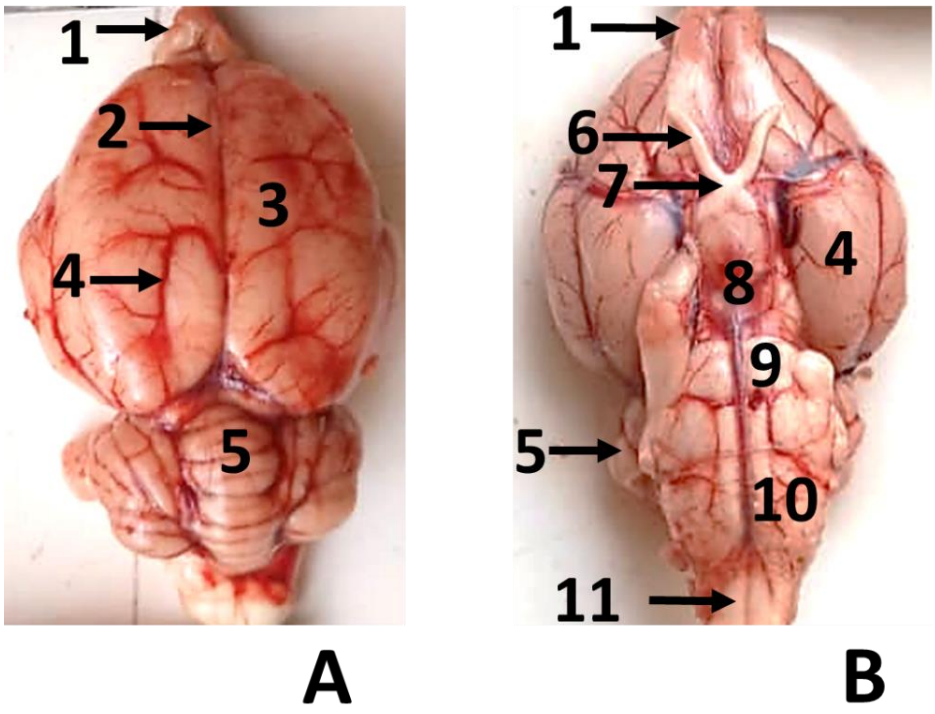

Figure 5: Brain of the African grasscutter

A: Dorsal view; **B**: Ventral view; **1**: Olfactory bulb; **2**: Sagittal (intercerebral) fisure, separating the cerebral hemispheres; **3**: Cerebrum (right hemisphere); **4**: Sulcal depression; **5**: Cerebellum; **6**: Optic tract; **7**: Optic chiasma; **8**: Midbrain; **9**: Pons; **10**: Medulla; **11**: Spinal cord.

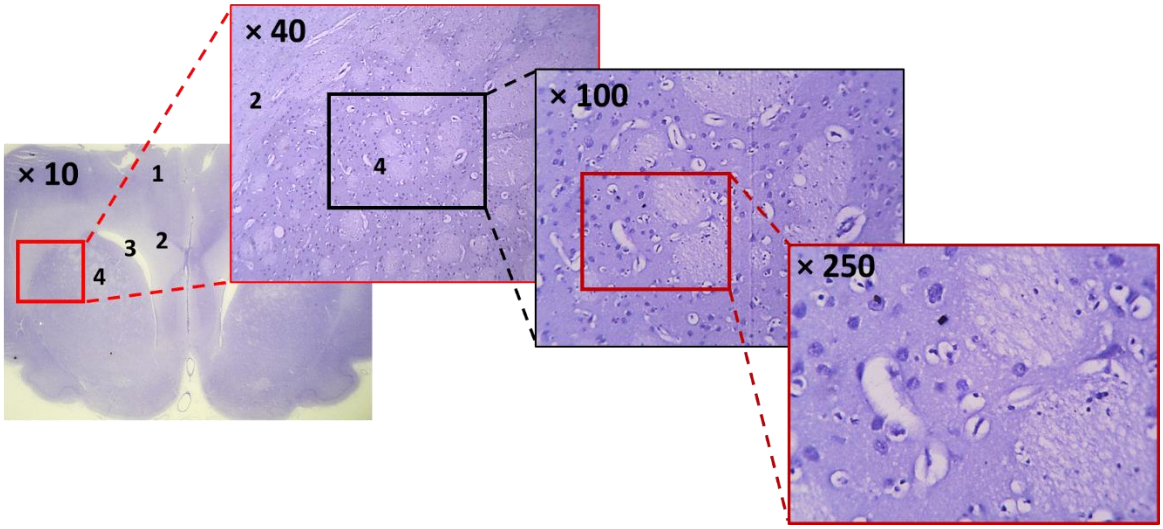

Figure 6: Coronal section of African grasscutter brain with the caudate putamen. CFV stain

1: Cerebral cortex; **2**: Corpus callosum; **3**: Lateral ventricle; **4**: Caudate putamen.

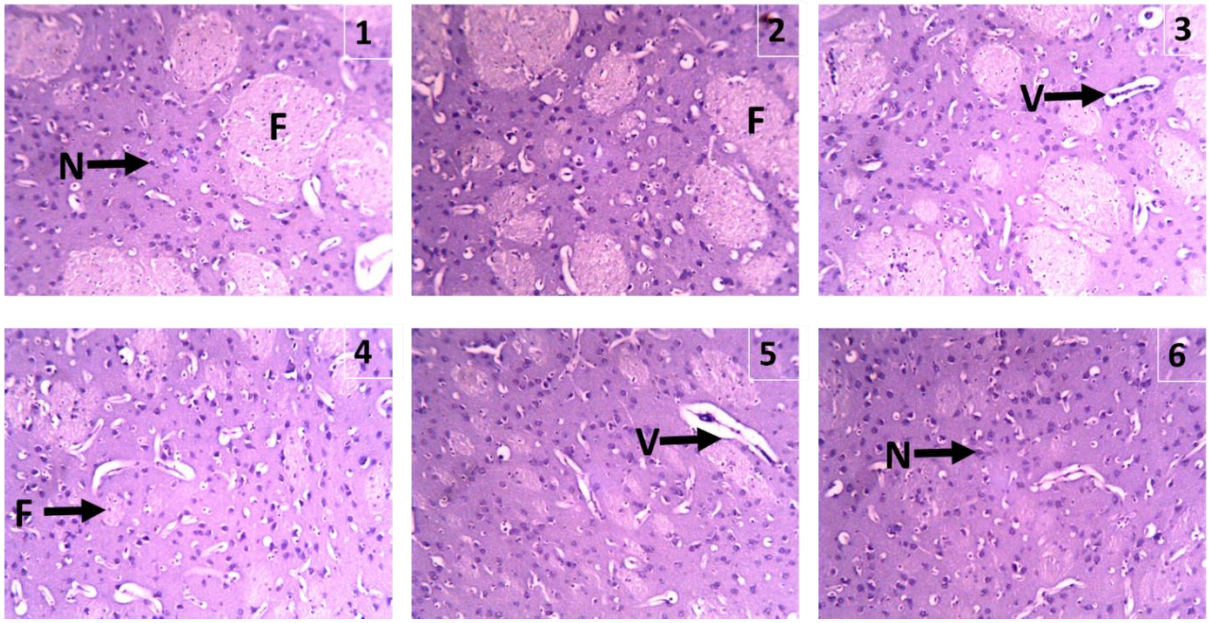

Figure 7: Section of the caudate putamen of African grasscutter. ×100 H&E.

1: Superomedial; **2**: Superolateral; **3**: Mediomedial; **4**: Mediolateral; **5**: Inferomedial; **6**: Inferolateral; **N**: Neuronal cell; **F**: Funiculus (white mater); **V:** Blood vessel (capillary).

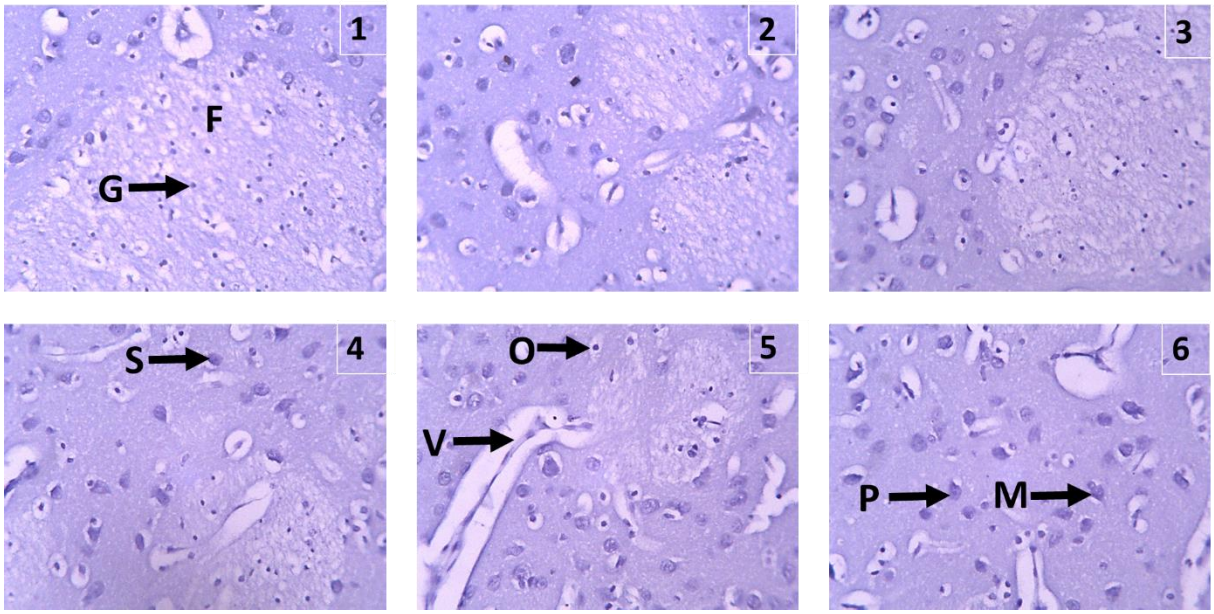

Figure 8: Sections of the caudate putamen of African grasscutter. ×250 CFV stain.

1: Superomedial; **2**: Superolateral; **3**: Mediomedial; **4**: Mediolateral; **5**: Inferomedial; **6**: Inferolateral **F:** Fasciculus; **G**: Glial cell; **M:** Multipolar cell **P**: Pyramidal Cell; **O:** Oligodendrocyte; **S**: Stellate cell; **V**: Blood vessel (capillary).

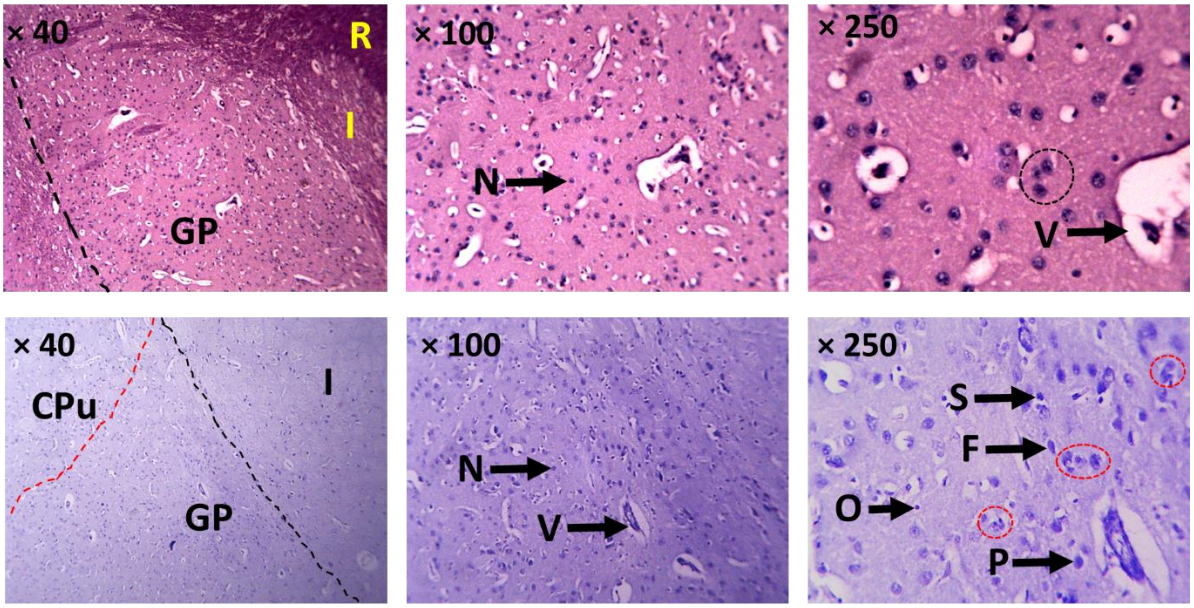

Figure 9: Sections of the globus pallidus of African grasscutter. H&E (top row) and CFV (bottom row) stains.

F: Fusiform cell; **P**: Pyramidal cell; **O**: Oligodendrocyte; **V:** Blood vessel; **CPu**: Caudate putamen; **GP**: Globus pallidus; **I**: Internal capsule; **R:** Reticular thalamic nucleus; **Red oval broken line**: Neuronal synapses in the GP.

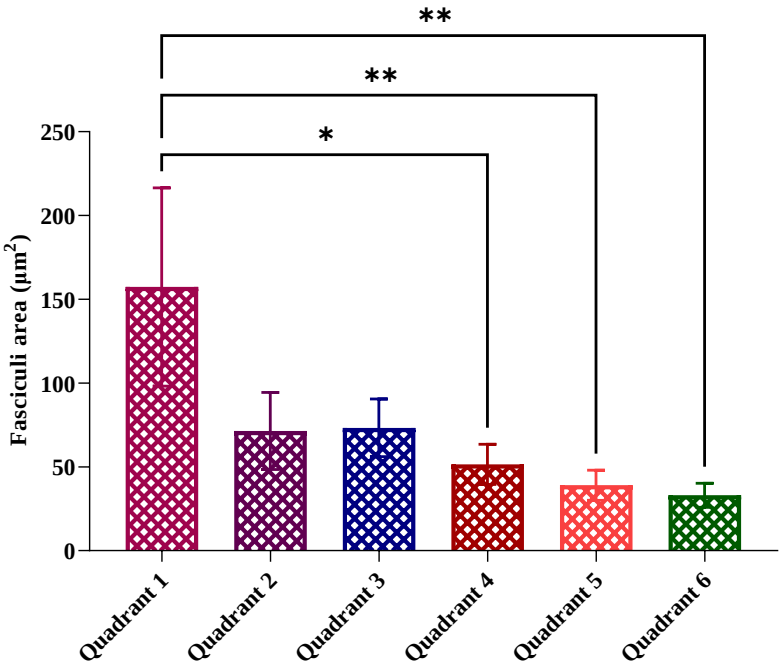

Figure 10: Histometric characteristic of fasciculi (area) of African grasscutter

n= 4, mean ± SEM, one-way ANOVA, *Tukey post hoc* test, *=p<0.05 when quadrant 1 was compared to quadrant 4, **=p<0.05 when quadrant 1 was compared to quadrants 5 and 6.

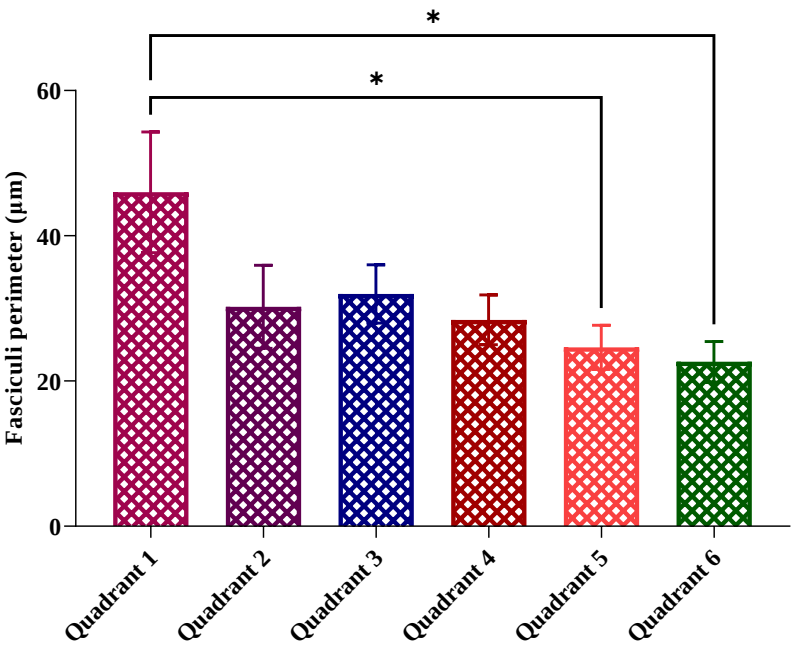

Figure 11: Histometric characteristic of fasciculi (perimeter) of African grasscutter

n= 4, mean ± SEM, one-way ANOVA, *Tukey post hoc* test, *=p<0.05 when quadrant 1 was compared to quadrants 5 and 6

DISCUSSION

In this study, AGC brain morphologic features were described and the striatal features characterized using histological, hisctochemical, and histometric approaches.

The observed mean AGCs' absolute body weight value greater than 2 kg is in lined with reported values for adults AGCs. [39] This placed the species as a large rodent; larger than the African giant rat (*Cricetomys gambianus*) with reported mean absolute body weight > 1 kg [40] for adults, but less weighty than some rodent species including porcupine with reported mean absolute body weight > 7 kg. [41] The milky coloration of the AGCs brain is in agreement with reported brain coloration for rodent species. [42] [43] [44] This coloration is a common manifestation of structures of the central nervous system linked with the presence of an integral biochemical component, lipid moieties. [45] [46]

Major sulcal depressions delineating the cerebrum from cerebellum and, separating the two cerebral hemispheres observed in this rodent species agrees with the reported characteristics of the brain of rodents. [42] [47] [48] Grooves (minor sulcal depressions) observed on the dorsal surface of the cerebrum suggests the species to be gyrencephalic. This finding agrees with reported gyrencephalic cortex in some rodents including the agoutis and guinea pigs having certain patterns of gyri on cortical cerebral surfaces. [49] [50] However, this finding is at variance with the commonly reported lissencephalic cerebral cortex for rodents. [37] This variance could be associated to adaptive variation in this species, AGC, and/ or probably influenced by factors including environment and genetics. [49] Morphologic features of the ventral surfaces including brain stem observed in this rodent species is in lined with reported characteristics in rodents and other mammalian species. [40] [51]

The mean brain weight of AGCs observed to be > 12 g agreed with reported mean values for adults AGCs. [39] [47] This mean brain weight value is greater than that reported for murine, hamsters, squirrel, [52] guinea pigs [42] and African giant rats. [39] [53] Brain size in the mammalian species tends to increase with increasing cranial cavity. In this study, measured brain dimensions (total brain, cerebral and cerebellar parameters) of the AGC suggest this trend with values comparatively higher than that reported in some rodent species including rats, guinea pigs and African giant rats. [87] Olude et al., [53] and Ibe et al., [47] reported a significant difference in brain dimensions for different brain weights of rodent species across age groups. This finding agrees with reports that attributed larger brain dimensions to brain weights in different species. [42] [43]

Microscopically, the histoarchitectural features of the AGCs CPu as bilateral oval shaped subcortical nuclei, just dorsal to the corpus callosum is characteristic of the mammalian species including rodents. [54] [55] [56] Developmentally, striatal elements arise as deep telencephalic structures on both sides of the cerebral hemispheres. [57] [58]

The observed varying neuronal and glial cell types is a common feature of neuronal tissue. Neuronal cells are the main cellular components of the nervous tissues, and the glial cells are supporting components. [59] [60] The fasciculi as patches of white mater

(reticulations) imply neuronal connectivity with bilaterally similar (commissural fibers) and different (ipsilateral and/ or contra-lateral; association fibers/ projections) regions of the brain. [61] [62] [63] Wouterlood et al., [64], have demonstrated several striatal connections to and from different regions of the brain. This CPu characteristic parenchymal features having neuronal and glial cellular components mingling with reticulations is in line with striatal histoarchitectural patterns reported in mammalian species including rodents such as mice and rats. [55] [54] The accompanying blood capillaries peripheral to the reticulations within the AGCs CPu shows a typical vascularized tissue similarly reported in mammalian species. [65] [66]

Histochemically, the characteristic architecture of the white mater patches (reticulations; fascicules) delineated as an oval to circular shaped feature of AGCs CPu suggests glial-outlined bundles of white mater participating in striatal connectivity with different regions of the brain including cortical and subcortical nuclei. Gerfen and Surmeier, [67] demonstrated that, the CPu received excitatory corticostriatal and thalamic tracts as direct input. The variations in fascicular sizes and abundance in the defined quadrants of CPu of AGCs suggest regional compartmentalization probably associated with functional connectivity. Gerfen and Surmeier, [67], and Fujiyama et al., [68] demonstrated tracts both commissural and association fibers output directly to the GP and substantia nigra pars reticulate.

Varying cell morphologies observed in AGCs CPu including stellate, pyramidal, horizontal, multipolar, and fusiform cells are typical of nervous tissues presenting with morphologically distinct cell types that are functionally related. [69] [73] Planert et al. [72] and Oorschot [70] [71] reported difference neuronal cell morphologies in mammals including primate and non-primate species, especially rodents; mice and rats. The presence of glial cells within the parenchyma and periphery of the fascicules indicates glial-delineated peripheral boundaries of reticulations (fasciculi) providing nutritive, supportive, and other regulatory functions in the CPu of this species (AGCs). Tennyson et al. [74] and Gerfen et al. [75] reported histochemical reactivity of developing neostriatal neurons of rabbits and transgenic mice to Horse radish peroxidase (HRP); however, CFV is an excellent neuronal, cell body-specific stain. The positive reactivity of CPu cells to the histochemical stain, CFV implies the cells are involved in normal physiological and biochemical processes necessary for nervous tissue function. [75]

The GP observed as a subcortical nuclei situated inferomedially to the CPu agrees with the reported location of GP as subcortical striatal elements in mammalian species including rodents. [76] [77] Striatal structures arise deep in the telencephalon during brain development and maintained same location at adulthood on either sides of the cerebral hemispheres. [78] [79] The varying neuronal cell types and glial cells observed in the parenchyma of GP is typical of cytoarchitecture of the nervous tissue. [59] [60] Pockets of clustered cells indicates neuronal and inter-neuronal synaptic communication which could be axo-somato-dendritic synapses; probably groups of functionally dependent neuronal cells. These communications could be inhibitory or excitatory regulating pallidal homeostasis. These findings are in line with

previous studies in mammals including rodents, that reported pockets of clustering cells in certain regions of the brain [38] [60] and associated these clustering formations as functionally interdependent neurons. Reactivity of GP cells to CFV stains is suggestive of the cells involvement in normal physiological and biochemical processes necessary for nervous tissue function. [80] [81]

The observed remarkable differences in fasciculi sizes (area and perimeter) within the defined six quadrants of AGCs' CPu with histometric quantification corroborate histological observations in this study. These variations in fascicular sizes, especially larger calibers in the medial quadrants of AGC CPu is suggestive of regional compartmentalization probably associated with certain and/ or specific connections between cortical and subcortical regions of the brain. Parent and Hazrati, [82] together with Stoessl et al., [83]; reported striatal connectivity ranging from commissural to projecting fibers from the cortical regions to the superomedial compartments of the CPu (corticostriatal); between the thalamus and striatum (thalamostriatal); between the substantia nigra and striatum (nigrostriatal), between the GP, and striatum (striatopallidal). [84] [85] [86]

The brain morphologic features of AGC demonstrate a relatively large brain for a rodent species with cortical cerebral sulcal depressions placing this species as gyrencephalic. Microscopic striatal and pallidal features characterize this species as having a typical architecture of the subcortical structures of mammalian central nervous system. Although, there is much to be elucidated about the neuroanatomy of this species owing to the methodologies adopted to characterize certain features of the basal nuclei of this species. However, it is convenient to mention that, these characteristic formations suggest a well-organized central nervous system with basal nuclei elements necessary for motor homeostatic functionality that relates to certain behavioral patterns for the survival of the species, AGC. Thus, the species is potentially beneficial in neuroscience investigations with clinical relevance ranging from movement disorders and therapy, motivation, reward and cognitive abilities.

CONCLUSION

The brain morphologic and striato-pallidal microscopic features of the *Thryonomys swinderianus* (African grasscutter, AGC) is typical for a rodent species. These findings present AGC as a potential model in neuroscience related investigations.

REFERENCES

1. Ferrier, D. The functions of the brain. *Smith, Elder, & Co, London*.1876.
2. David, S. *The Nervous System* in: An Introduction to functional Anatomy 5th Ed. 1975; pp.101-108.
3. Cazalis, M., Dayanithi, G. and Nordmann, J. J. The role of pattern burst and interburst interval on the excitation-coupling mechanism in the isolated rat neural lobe. *Journal of Physiology*, 1985; (369): pp. 45-60.
4. Williams, P.L. and Warwick, R. Gray's anatomy, *37th edition New York: Churchill Livingstone*. 1989.
5. Kandel, Eric R., Schwartz, James Harris, Jessell, Thomas M. Principles of Neural

Science *4th ed. New York; McGraw-Hill*. 2000.

6. Rueda-Orozco, P. E. & Robbe, D. The striatum multiplexes contextual and kinematic information to constrain motor habits execution. *Nat. Neurosci*. 2015;(18):453–460.
7. Middleton, F.A., Strick, P.L. Basal ganglia output and cognition: evidence from anatomical, behavioral, and clinical studies. Brain Cogn. 2000;(42):183–200.
8. Tai, L.-H., Lee, A. M., Benavidez, N., Bonci, A. & Wilbrecht, L. Transient stimulation of distinct subpopulations of striatal neurons mimics changes in action value. *Nat. Neurosci*. 2012;(15):1281–1289.
9. Kim, H. F., Hikosaka, O. Distinct basal ganglia circuits controlling behaviors guided by flexible and stable values. *Neuron*. 2013;(79): 1001–1010.
10. Wang, L., Rangarajan, K. V., Gerfen, C. R. & Krauzlis, R. J. Activation of striatal neurons causes a perceptual decision bias during visual change detection in mice. *Neuron*. 2018;(97):1369–1381.e5.
11. Guo, L., Walker, W. I., Ponvert, N. D., Penix, P. L., Jaramillo, S. Stable representation of sounds in the posterior striatum during flexible auditory decisions. *Nat. Commun*. 2018;(9) 1534.
12. Bishop, G.A., Chang, H.T., Kitai, S.T. Morphological and physiological properties of neostriatal neurons: an intracellular horse-radish peroxidase study in the rat. *Neuroscience*. 1982;(7): 179-191.
13. Wilson, C.J., Groves, P.M. Fine structure and synaptic connections of the common spiny neuron of the rat neostriatum: a study employing intracellular injection of horseradish peroxidase. *J. Comp. Neurol*. 1980;(194):599-615.
14. Joel, D., Weiner, I. The connections of the dopaminergic system with the striatum in rats and primates: an analysis with respect to the functional and compartmental organization of the striatum. *Neuroscience*. 2000;(96):451–474.
15. Wilson, C.J., Phelan, K.D. Dual topographic representation of neostriatum in the globus pallidus of rats. *Brain Res*. 1982; (243):354-359.
16. Kincaid, A. E., Zheng, T. & Wilson, C. J. Connectivity and convergence of single corticostriatal axons. *J. Neurosci*. 1998;(18): 4722–4731.
17. Huerta-Ocampo, I., Mena-Segovia, J., Bolam, J. P. Convergence of cortical and thalamic input to direct and indirect pathway medium spiny neurons in the striatum. *Brain Struct. Funct*. 2014;(219):1787–1800.
18. Fisher HE, Aron A, Brown LL. Romantic love: a mammalian brain system for mate choice. *Philos Trans R Soc Lond B Biol Sci*. 2006 Dec 29;361(1476):2173-86. [PMC free article] [PubMed]
19. Grahn JA, Parkinson JA, Owen AM. The cognitive functions of the caudate nucleus. *Prog Neurobiol*. 2008 Nov;86(3):141-55. [PubMed]
20. Yartsev, M. M., Hanks, T. D., Yoon, A. M., Brody, C. D. Causal contribution and dynamical encoding in the striatum during evidence accumulation. *eLife* 2018;(7): e34929.
21. Peters, A.J., Fabre, J.M.J., Steinmetz, N.A., Harris, K.D., Carandini, M. Striatal activity topographically reflects cortical activity. Nature 2021;(591): 420–425.

https://doi.org/10.1038/s41586-020-03166-8

22. Bolkan, S.S., Stone, I.R., Pinto, L., Ashwood, Z.C., Iravedra Garcia, J.M., Herman, A.L., Singh, P., Bandi, A., Cox, J., Zimmerman, C.A., et al. Opponent control of behavior by dorsomedial striatal pathways depends on task demands and internal state. *Nat. Neurosci*. 2022;(25):345–357. https://doi.org/10.1038/s41593-022-01021-9
23. Lau, B., Glimcher, P.W. Value representations in the primate striatum during matching behavior. *Neuron.* 2008;(58):451–463. https://doi.org/10.1016/j.neuron.2008.02.021.
24. Bradfield, L.A., Bertran-Gonzalez, J., Chieng, B., Balleine, B.W. The thalamostriatal pathway and cholinergic control of goaldirected action: interlacing new with existing learning in the striatum. *Neuron* 2013;(79):153–166. https://doi.org/10.1016/j.neuron.2013.04.039.
25. Okada, K., Nishizawa, K., Fukabori, R., Kai, N., Shiota, A., Ueda, M., Tsutsui, Y., Sakata, S., Matsushita, N., and Kobayashi, K. Enhanced flexibility of place discrimination learning by targeting striatal cholinergic interneurons. *Nat. Commun.* 2014;(5):3778. https://doi.org/10.1038ncomms4778
26. Matamales, M., Skrbis, Z., Hatch, R.J., Balleine, B.W., Go¨ tz, J., Bertran-Gonzalez, J. Aging-related dysfunction of striatal cholinergic interneurons produces conflict in action selection. *Neuron*. 2016;(90):362–373. https://doi.org/10.1016/j.neuron.2016.03.006.
27. Manger, P.R. Establishing order at the systems level in mammalian brain evolution. *Brain Res. Bull.* 2005;(66) 282–289.
28. Fayenuwo JO., Modupe Akande, Taiwo, A. A. "Guidelines for Grasscutter rearing. *Technical Bulletin, IAR and T, Ibadan"* 2003; 38.
29. Van der Merwe, M. Discriminating between Thryonomys swinderianus and Thryonomys gregorianus. *African Zoology*. 2007;(42):165—171.
30. Asibey, E.O.A., Addo, P.G. The grasscutter, a promising animal for meat production. In Turnham, D.: African Perspectives. Practices and Policies Supporting Sustainable Development. Scandinavian Seminar College, Denmark, in association with Weaver *Press, Harare, Zimbabwe.* 2000;120 pp
31. Onebunne, A. Grasscutter Farming — the Pathway to Wealth. In http://grasscutterfarmingbest.blogspot.com. 2010; Accessed: 16:08:2014. 16:07:27 GMT
32. Adkins, R.M., Walton, A.H., Honeycutt, R.L. Higher-level systematics of rodents and divergence time estimates based on two congruent nuclear genes. *Mol. Phylogenet. Evol*. 2003;(26):409–420.
33. Aluko FA. "Qualitative characteristics of Thryonomys swinderianus swinderianus and Thryonomys swinderianus gregorianus". *Nigerian Journal Animal Production*. 2014;41(1): 258-263.
34. Enemali Felix Udawnojo., Iteire Kingsley Afoke, Uweijigho Raphael, Oladele Tolulope Samuel, Agbon Abel N., Emmanuel I. Odokuma. "Identification of Neuronal cell types and Immunohistochemical Localisation of Dopaminergic Neurons in the Spinal Cord Segment of Grasscutter

(Thryonomys Swinderianus)". *Acta Scientific Anatomy*. 2022;1(6):11-15

35. Mensah, G.A., Okeyo, A.M. Continued harvest of the diverse African animal genetic resources from the wild through domestication as a strategy for sustainable use: A case of the larger grasscutter: Thryonomys swinderianus. In http://agtr.ilri. cgiar.org/index.php?option=com_content&task=view&id=177 &Itemid=199. 2005; Accessed: 27/10/2012, 23: 12: 34 GMT.
36. Ibe, C.S., Salami, S. O., Wanmi, N. Brain size of the African Grasscutter (Thryonomys swinderianus TEMMINCK-1827) at defined postnatal periods. *Folia Vet.* 2017;6(4):5-11.
37. Gage, G.J., Kipke, D.R., Shan, W. Whole animal perfusion fixation for rodents. *JVE.* 2012;65: e3564.
38. Agbon A.N., Ahmad A.N., Mahdi O., Bobbo, K.A., Bala, U., Enemali F. U., Henry, R., Shuaib Y. M., Yusha U. Z. Neuroanatomical Studies on the Tectum of some Selected Rodent Species. *J. Anat Sci*. 2022;13 (2): 1-12.
39. Byanet O, Dzenda T. Quantitative biometry of body and brain in the grasscutter (Thryonomys swinderianus) and African giant rat (Cricetomys gambianus): Encephalization quotient implication. *Research in Neuroscience.* 2014;3(1):1-6.
40. Olude MA, Mustapha OA, Olopade JO. Morphological Characterization of the African Giant Rat (Cricetomys gambianus, Waterhouse) Brain Across Age Groups: Gross Features of Cortices. *Niger. J. Physiol Sci*. 2017;31(2):133-8.
41. Fournier F, Thomas DW. Nitrogen and energy requirements of the North American porcupine (Erethizon dorsatum). *Physiological zoology*. 1997;70(6):615-20.
42. Musa SA, Yahaya FM, Omoniyi AA, Timbuak JA, Ibegbu AO. Comparative Anatomical Studies of the Cerebrum, Cerebellum,and Brainstem of Males Guinea pig (Cavia porcellus) and Rabbit (Oryctolagus cuniculus). *Journal of Veterinary Anatomy*. 2016;9(2):1-14.
43. Ibegbu AO, Yahaya BO, Adubazi P, Musa SA. Comparative Histomorphologic Studies of the Heart in Three Mammalian Species: Rabbits (Oryctolagus guniculus), Wistar Rats (Rattus norvegicus) and African Giant Rats (Cricetomys gambianus). *Journal of Veterinary Anatomy*. 2014;7(2):101-16.
44. Dwarika, S., Maseko, B. C., Ihunwo, A. o., Manger, P. A., Distribution and morphology of putative catecholaminergic and serotonergic neurons in the greater canerat, Thryonomys swinderianus. *Journal of chem. Neuroanatomy*. 2008;35 108-122.
45. Poon KW, Brideau C, Klaver R, Schenk GJ, Geurts JJ, Stys PK. Lipid biochemical changes detected in normal appearing white matter of chronic multiple sclerosis by spectral coherent Raman imaging. Chemical science. 2018;9(6):1586-95.
46. Aschner M, Toews AD. Myelin and myelination. Nervous System and Behavioral Toxicology: *Elsevier Inc.* 2010. p. 181-98.
47. Ibe CS, Salami SO, Wanmi N. Brain size of the African grasscutter (Thryonomys swinderianus, Temminck, 1827) at defined postnatal periods. *Folia Vet.* 2017; (61):5-11.
48. Pardo ID, Rao DB, Morrison JP, Huddleston C, Bradley AE, Bolon B, et al. Nervous system sampling for general

toxicity and neurotoxicity studies in rabbits. *Toxicologic Pathology*. 2020;48(7):810-26.
49. Hatakeyama J, Sato H, Shimamura K. Developing guinea pig brain as a model for cortical folding. *Development, Growth & Differentiation*. 2017;59(4):286-301.
50. García-Moreno F, Vasistha NA, Trevia N, Bourne JA, Molnar Z. Compartmentalization of cerebral cortical germinal zones in a lissencephalic primate and gyrencephalic rodent. *Cerebral cortex*. 2012;22(2):482-92.
51. Ibe CS, Ezeifeka AC, Ikpegbu E. Anatomical Demonstration of the Cognitive Ability of the Juvenile African Giant Pouched Rat (Cricetomys gambianus-Waterhouse, 1840). 2021.
52. Bolon B, Graham DG. Appendixes: Ready References of Neurobiology Knowledge. *Fundamental Neuropathology for Pathologists and Toxicologists: Principles and Techniques*. 2011:541- 8.
53. Olude MA, Mustapha OA, Olopade JO. Morphological characterization of the African Giant Rat (Cricetomys gambianus, Waterhouse) brain across age groups: Gross features of cortices. *Nigerian Journal of Physiological Sciences*. 2016;31(2):133-8.
54. Graybiel, A.M., Ragsdale Jr., C.W. Histochemically distinct compartments in the striatum of human, monkeys, and cat demonstrated by acetylthiocholinesterase staining. *Proc. Natl. Acad. Sci. U.S.A.* 1978;(75):723-5726.
55. Gerfen, C.R. The neostriatal mosaic: multiple levels of compartmental organization in the basal ganglia. *Annu. Rev. Neurosci.* 1992;(15):285-320.
56. Pellizzaro Venti M, Paciaroni M, Caso V. Caudate infarcts and hemorrhages. *Front Neurol Neurosci*. 2012;(30):137-40. [PubMed]
57. Onorati M, Castiglioni V, Biasci D, Cesana E, Menon R, Vuono R, Talpo F, Laguna Goya R, Lyons PA, Bulfamante GP, Muzio L, Martino G, Toselli M, Farina C, Barker RA, Biella G, Cattaneo E. Molecular and functional definition of the developing human striatum. *Nat Neurosci*. 2014 Dec;17(12):1804-15. [PubMed]
58. Dayer AG, Cleaver KM, Abouantoun T, Cameron HA. New GABAergic interneurons in the adult neocortex and striatum are generated from different precursors. *J Cell Biol*. 2005 Jan 31;168(3):415-27. [PMC free article] [PubMed]
59. Walz, W. Role of glial cells in the regulation of the brain ion microenvironment. *Prog. Neurobiol*. 1989;(33):309-333.
60. White, H.S., Chow, S.Y., Yen-Chow, Y.C., Woodbury, D.M., Effect of elevated potassium on the ion content of mouse astrocytes and neurons. Can. *Physiol. Pharmacol*. 1992;(70): S263-S268.
61. Müller NCJ, Konrad BN, Kohn N, Muñoz-López M, Czisch M, Fernández G, Dresler M. Hippocampal-caudate nucleus interactions support exceptional memory performance. *Brain Struct Funct*. 2018 Apr;223(3):1379-1389. [PMC free article] [PubMed]
62. Hasegawa H, Matsuura M, Sato H, Yamamoto T, Kanai H. Imaging of gaps in digital joints by measurement of ultrasound transmission using a linear array. *Ultrasound Med Biol*. 2009 Mar;35(3):382-94. [PubMed]

63. Grahn JA, Parkinson JA, Owen AM. The cognitive functions of the caudate nucleus. *Prog Neurobiol.* 2008 Nov;86(3):141-55. [PubMed]
64. Wouterlood, F.G., Hartig, W., Groenewegen, H.J., Voorn, P. Density gradients of vesicular glutamate- and GABA transporter-immunoreactive boutons in calbindin and μ-opioid receptor defined compartments in the rat striatum. *J. Comp. Neurol.* 2012;(520): 2123-2142.
65. Tatu L, Moulin T, Bogousslavsky J, Duvernoy H. Arterial territories of the human brain: cerebral hemispheres. *Neurology.* 1998 Jun;50(6):1699-708. [PubMed]
66. Feekes JA, Cassell MD. The vascular supply of the functional compartments of the human striatum. *Brain.* 2006 Aug;129(Pt 8):2189-201. [PubMed]
67. Gerfen, C.R., Surmeier, D.J., Modulation of striatal projection systems by dopamine. *Annu. Rev. Neurosci.* 2011;(34):441-466.
68. Fujiyama, F., Sohn, J., Nakano, T., Furuta, T., Nakamura, K.C., Matsuda, W., Kaneko, T., Exclusive and common targets of neostriatofugal projections of rat striosome neurons: a single neuron-tracing study using a viral vector. *Eur. J. Neurosci.* 2011;(33):668-677.
69. Mingazzini, G. Sulla fine struttura della Substantia nigra So¨mmeringii. Reale Acad. Lincei *(Roma).* 1888;(5) 36-40
70. Oorschot, D.E. The domain hypothesis: a central organising principle for understanding neostriatal circuitry? In: Miller, R., Wickens, J.R. (Eds.), Conceptual Advances in Brain Research, Brain Dynamics and the Striatal Complex. *Gordon and Breach, Reading, UK.* 2000; pp. 151-163.
71. Oorschot, D.E. The percentage of interneurons in the dorsal striatum of the rat, cat, monkey and human: a critique of the evidence. *Basal Ganglia.* 2013;(3):19-24.
72. Planert, H., Szydlowski, S.N., Hjorth, J.J.J., Grillner, S., Silberberg, G. Dynamics of synaptic transmission between fast-spiking interneurons and striatal projection neurons of the direct and indirect pathways. *J. Neurosci.* 2010;(30):3499-3507.
73. Oorschot D. E. Total number of neurons in the neostriatal, pallidal, subthalamic, and substantia nigra nuclei of rat basal ganglia: a stereological study using the cavalieri and optical dissector methods, *J. Comp. Neurol.* 1996;(366):580-599.
74. Tennyson, V.M., Barrett, R.E., Cohen, G., Coˆte´, L., Heikkila, R., Mytilineou, C. The developing neostriatum of the rabbit: correlation of fluorescence histochemistry, electron microscopy, endogenous dopamine levels, and (3H) dopamine uptake. *Brain Res.* 1972;(46):251-285.
75. Gerfen, C.R., Paletzki, R., Heintz, N., GENSAT BAC cre-recombinase driver lines to study the functional organization of cerebral cortical and basal ganglia circuits. *Neuron.* 2013;(80):1368-1383.
76. Grillner, S., Robertson, B., Stephenson-Jones, M. The evolutionary origin of the vertebrate basal ganglia and its role in action selection. *J. Physiol.* 2013;591(22): 5425-5431
77. Tepper, J.M., Abercrombie, E.D., Bolam, J.P. Basal ganglia macrocircuits. *Prog. Brain Res.* 2007;(160):3-7.
78. Mortazavi MM, Adeeb N, Griessenauer CJ, Sheikh H, Shahidi S, Tubbs RI, Tubbs RS. The ventricular system of the brain: a comprehensive review of its history, anatomy, histology,

embryology, and surgical considerations. *Childs Nerv Syst.* 2014 Jan;30(1):19-35. [PubMed]

79. Fazl A, Fleisher J. Anatomy, Physiology, and Clinical Syndromes of the Basal Ganglia: *A Brief Review*. *Semin Pediatr Neurol*. 2018 Apr;25:2-9. [PMC free article] [PubMed]
80. Mallet, N., Micklem, B.R., Henny, P., Brown, M.T., Williams, C., Bolam, J.P., Nakamura, K.C., Magill, P.J. Dichotomous organization of the external globus pallidus. *Neuron*. 2012;(74):1075-1086.
81. Agbon AN, Kwanashie HO, Hamman WO, Ibegbu AO, Henry R, Sule H, et al. Comparative Microscopic Assessments of the Effect of Aqueous and Ethanol Extracts of Phoenix dactylifera L. in a Rat Model of Mercury-Triggered Hippocampal Changes. *Nigerian Journal of Physiological Sciences.* 2021;36(1):91-100.
82. Parent, A., Hazrati, L.-N., 1995. Functional anatomy of the basal ganglia. I. The cortico-basal ganglia-thalamo-cortical loop. *Brain Res. Rev.* 20, 91-127.
83. Stoessl, A.J., Lehericy, S., Strafella, A.P. Imaging insights into basal ganglia function, Parkinson's disease, and dystonia. *Lancet.* 2014;(384):532-544.
84. Kotz SA, Anwander A, Axer H, Knösche TR. Beyond cytoarchitectonics: the internal and external connectivity structure of the caudate nucleus. *PLoS One*. 2013;8(7): e70141. [PMC free article] [PubMed]
85. Mailly, P., Aliane, V., Groenewegen, H.J., Haber, S.N., Deniau, J.M. The rat prefrontal system analyzed in 3D: evidence for multiple interacting functional units. *J. Neurosci.* 2013;(33):5718-5727
86. McFarland, N.R., Haber, S.N. Thalamic relay nuclei of the basal ganglia form both reciprocal and nonreciprocal cortical connections, linking multiple frontal cortical areas. *J. Neurosci*. 2002;(22):8117-8132.
87. Agbon, A.N., Yusha, Z., Mahdi, O., Henry, R., Bobbo, K.A., Shuaib, Y. M., Enemali, F. U., Mesole, B. S., Usman, I. M., Ivang, A.E. Comparative Neuroanatomical characterization of the cerebrum of selected Rodents Species. *J Morphol. Sci*. 2023; 40:77-88